7

Microstructural Changes of Al-Cu Alloys After Prolonged Annealing at Elevated Temperature

Małgorzata Wierzbińska and Jan Sieniawski
Rzeszow University of Technology, Rzeszow, Poland

1. Introduction

The precipitation–strengthened 2xxx series Al–Cu alloys are one of the most important high-strength aluminium alloys. They have been employed extensively in the aircraft and military industries, in which materials are frequently subjected to elevated temperature. The aluminium casting alloys, based on the Al–Cu system are widely used in light–weight constructions and transport applications requiring a combination of high strength and ductility.

Al-Cu alloys are less frequently used than Al-Si-Cu grades due to technological problems in production process (e.g. high propensity to microcracking during casting). However they are the basis for development of multicomponent alloys. Typical alloys for elevated temperature application are Al-Cu-Ni-Mg alloys (containing about 4,5% Cu, 2% Mg and 2%Ni). Their good properties at elevated temperature result from formation of intermetallic phases Al_6Cu_3Ni and Al_2CuMg, both during crystallization and precipitation hardening (El–Magd & Dünnwald, 1996; Martin, 1968; Mrówka-Nowotnik et al., 2007).

Mechanism of precipitation hardening in cast and wrought binary Al-Cu alloys is well known and widely covered in literature. There are some suggestions that decomposition of supersaturated α(Al) solid solution in other precipitation hardened alloys like Al-Cu-Mg, Al-Si-Cu, Al-Mg-Si follows the same route as in the Al-Cu alloys with some specific features of the particular stages of the process (Martin, 1968;). The interest in course and kinetics of the aging process has the practical meaning as the early stages of aging leads to significant improvement of mechanical properties of the alloys. Maximum hardening effect in Al-Cu alloy is a result of in situ transformation of GP zones into transient phase θ''. Increase in aging temperature leads to decrease of the hardness of solid solution α(Al) due to precipitation of equilibrium θ phase on the grain boundaries or on the θ'/matrix phase boundaries. Prolonged aging may lead to microstructure degradation related to coagulation and/or coalescence of the highly dispersed hardening phase precipitates resulting in decrease of hardening effect (Mrówka-Nowotnik et al., 2007; Wierzbińska & Sieniawski, 2010). Therefore development of the chemical composition of the alloy, especially intended for long term operation at elevated temperature, requires taking into account factors resulting in deceleration of the coagulation process and obtaining stable microstructure consisting of solid solution α grains and highly dispersed precipitates of the second phase (Wierzbińska & Sieniawski, 2010).

2. Material and methodology

The investigation was performed on the two casting alumium alloys AlCu4Ni2Mg and AlCu6Ni. AlCu4Ni2Mg is the standard alloy used currently for highly stressed structural elements of engines and AlCu6Ni1 is an experimental alloy that was chosen to investigate the influence of the increased content of Cu on the phase composition, microstructure morphology and mechanical, technological and operational properties. The alloys were cast into metal moulds and subjected to X-ray inspection in order to exclude the presence of porosity or oxide films.

The alloys were subjected to heat treatment T6 followed by annealing at 523 K and 573 K for 150 and 500 hours. After analysis of the results of preliminary tests it was found, that it is advisable to apply additional annealing times at particular temperature, i.e. 100, 300 and 750 hours.

Heat treatment conditions were established on the basis of the phase equilibrium diagrams Al-Si and Al-Cu and available heat treatment data for the alloys with similar chemical composition (both from literature and used in industry practice). The consideration was also given to requirements concerning mechanical properties of the alloys resulting from operation condition of the structural elements made of these alloys. The chemical composition of the investigated alloys and heat treatment parameters are presented in table 1.

Element	Element content, wt.%	
	AlCu4Ni2Mg	AlCu6Ni
Mn	<0.10	0.90
Ni	2.10	1.10
Cu	4.30	6.36
Zr	–	0.01
Fe	0.10	0.20
Si	0.10	0.10
Mg	1.50	0.05
Zn	0.30	–
Al	balance	balance
solution treatment	$793^{\pm 5}$K/5h/ water cooling	$818^{\pm 5}$K/10h/ water cooling
artificial ageing	$523^{\pm 5}$K/5h/ air cooling	$498^{\pm 5}$K/8h/ air cooling

Table 1. Composition of AlCu4Ni2Mg and AlCu6Ni alloys and heat treatment parameters

Examination of the alloys microstructure was carried out using light microscope (LM), as well as scanning (SEM) and transmission (TEM) electron microscopes.

3. Results and discussion

Figs. 1 to 4 show the results of microscopic observations of AlCu4Ni2Mg and AlCu6Ni alloys (in T6 condition). In both of investigated alloys large, irregular shaped precipitates of

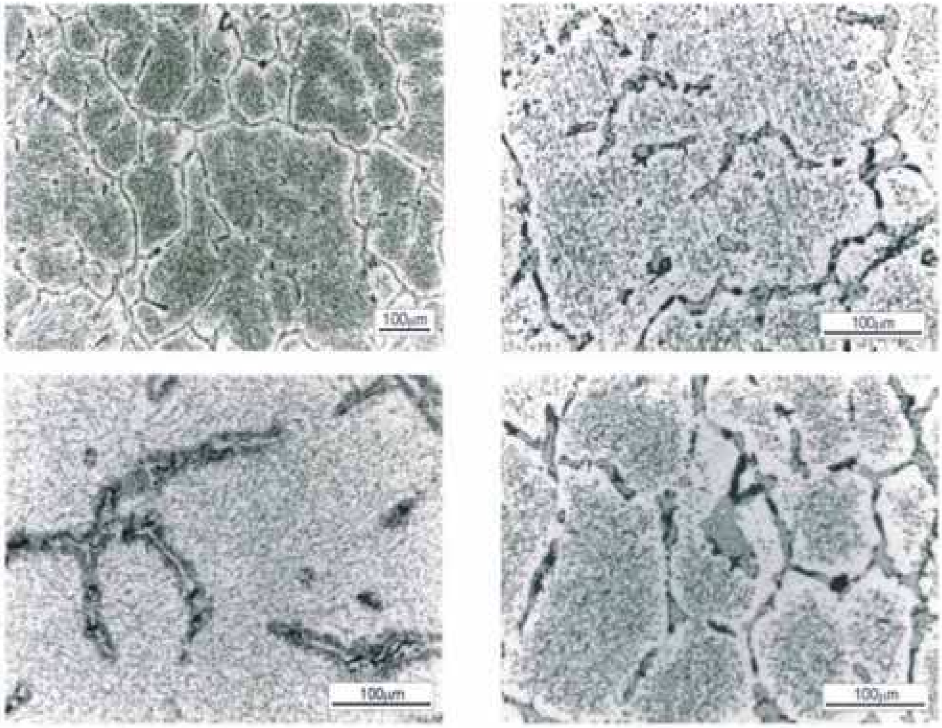

Fig. 1. Microstructure of AlCu4Ni2Mg alloy in T6 condition (LM)

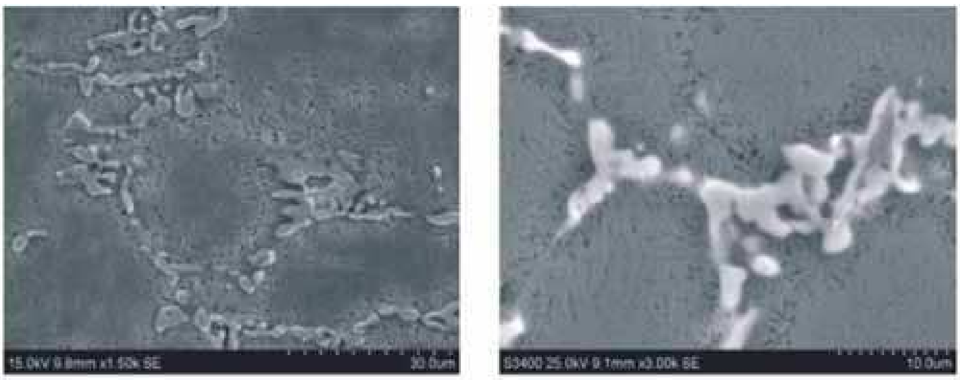

Fig. 2. Microstructure of AlCu4Ni2Mg alloy in T6 condition: precipitations of intermetallic phases in interdendritic areas (SEM)

intermetallic phases, located on the dendrite boundaries of solid solution α-Al and dispersive, spheroidal and strip shaped hardening phase precipitates homogenously distributed throughout the solid solution were observed.

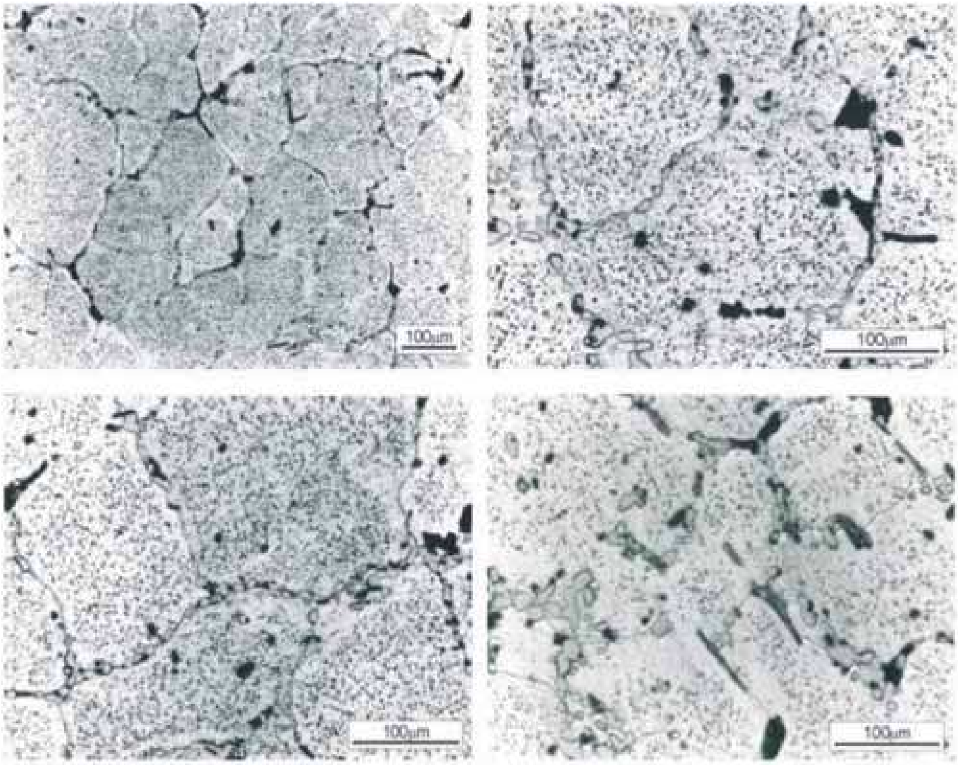

Fig. 3. Microstructure of the AlCu6Ni alloy in T6 condition (LM)

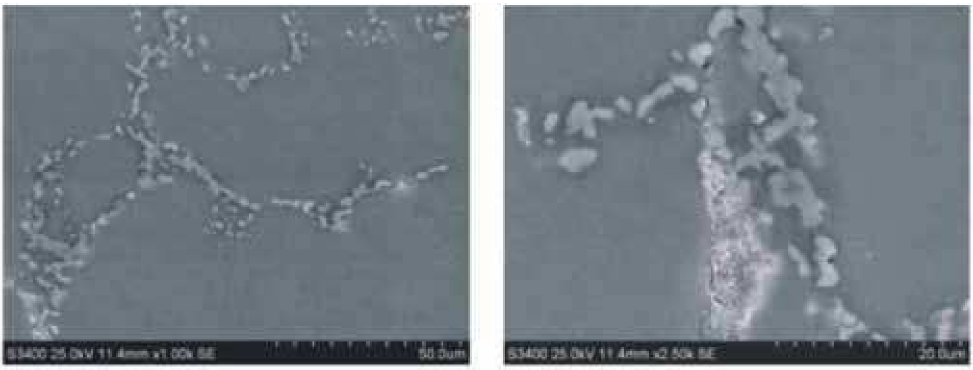

Fig. 4. Microstructure of the AlCu6Ni1 alloy in T6 condition (SEM)

Based upon the EDS results the phases forming large size particles was identified as Al-Cu-Ni, Al-Cu-Ni-Fe and Al-Cu-Mn (fig. 5–6) (Mrówka-Nowotnik et al. 2007, Wierzbińska & Sieniawski 2010).

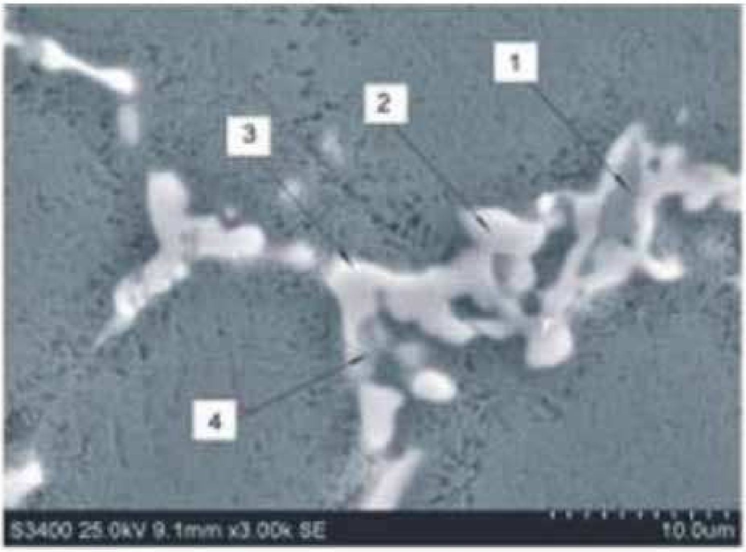

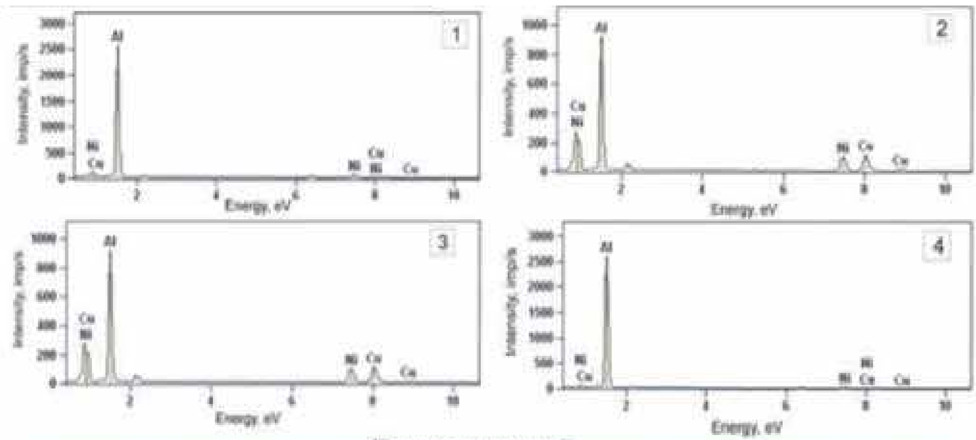

Element content, wt.%

	Al-K	Fe-K	Ni-K	Cu-K
AlCu4Ni2Mg – pt 1	76,32	5,95	13,39	4,35
AlCu4Ni2Mg – pt2	47,26		23,27	29,48
AlCu4Ni2Mg – pt 3	54,05		23,14	22,81
AlCu4Ni2Mg – pt 4	85,32	3,18	9,08	2,43

Fig. 5. AlCu4Ni2Mg alloy – EDS analysis of the areas 1–4

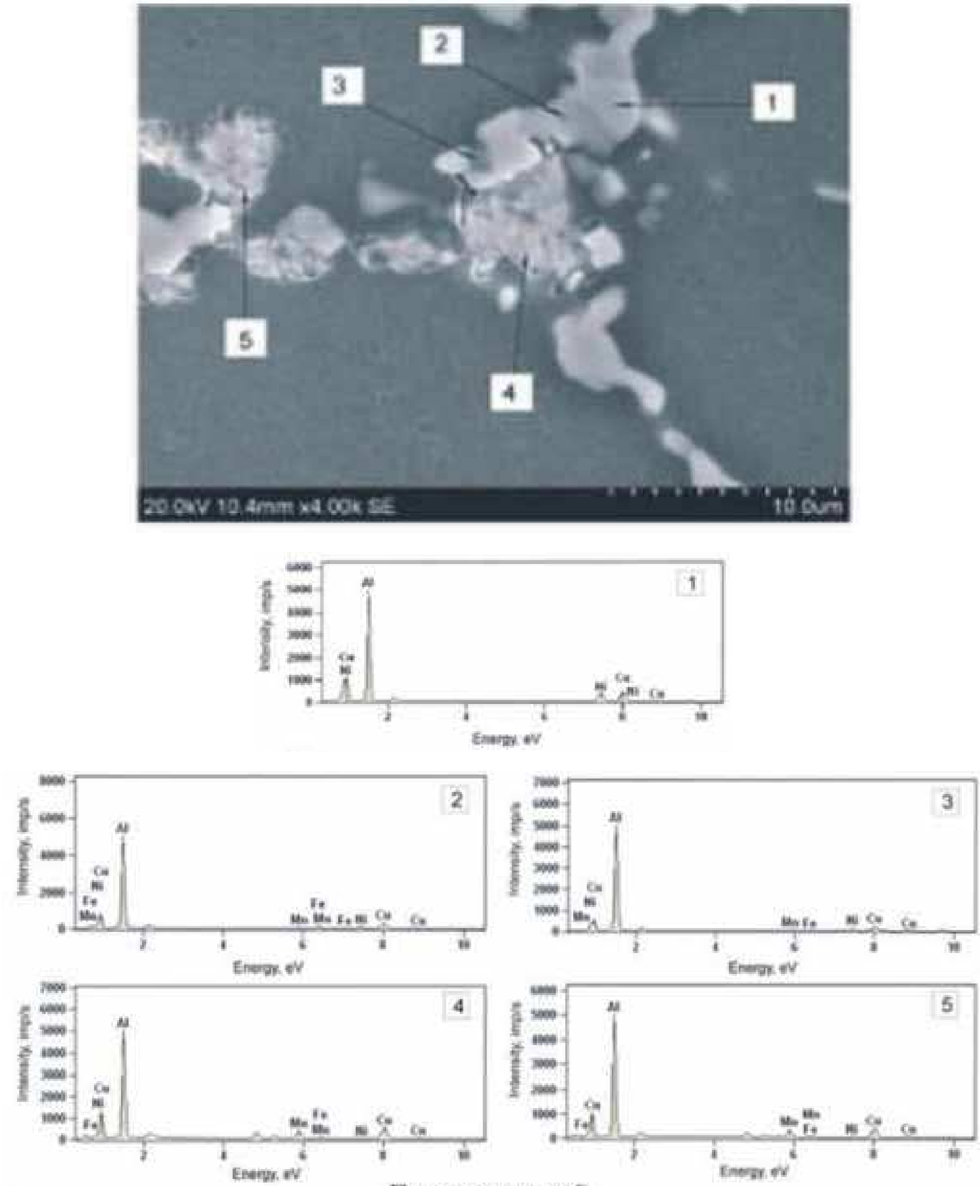

Element content, wt.%

	Al-K	Mn-K	Fe-K	Ni-K	Cu-K
AlCu6Ni1 - pt 1	53,07			19,43	27,51
AlCu6Ni1 - pt 2	60,00	2,38	4,65	6,68	26,29
AlCu6Ni1 - pt 3	65,90	3,94	1,29	8,44	20,43
AlCu6Ni1 - pt 4	51,14	10,42	1,19	2,24	35,02
AlCu6Ni1 - pt 5	55,12	10,06	1,87	2,19	30,76

Fig. 6. AlCu6Ni alloy – EDS analysis of the areas 1–5

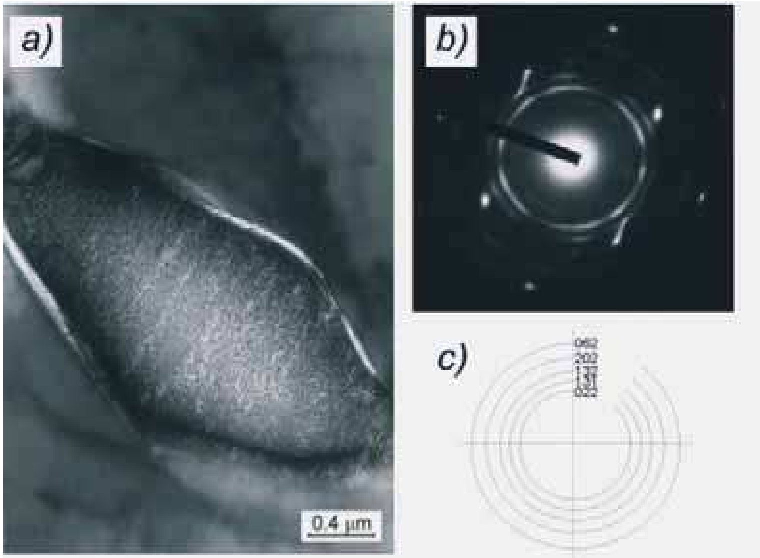

h k l	022	131	132	202	062
d (nm)	28,73	23,50	20,24	17,34	14,12
d (nm): S-Al_2CuMg	28,29	13,13	20,18	17,49	14,16

Fig. 7. Microstructure of the AlCu4Ni2Mg alloy: a) precipitates of *S-Al_2CuMg* phase, b) electron diffraction pattern obtained from the precipitate, c) solution of the diffraction pattern

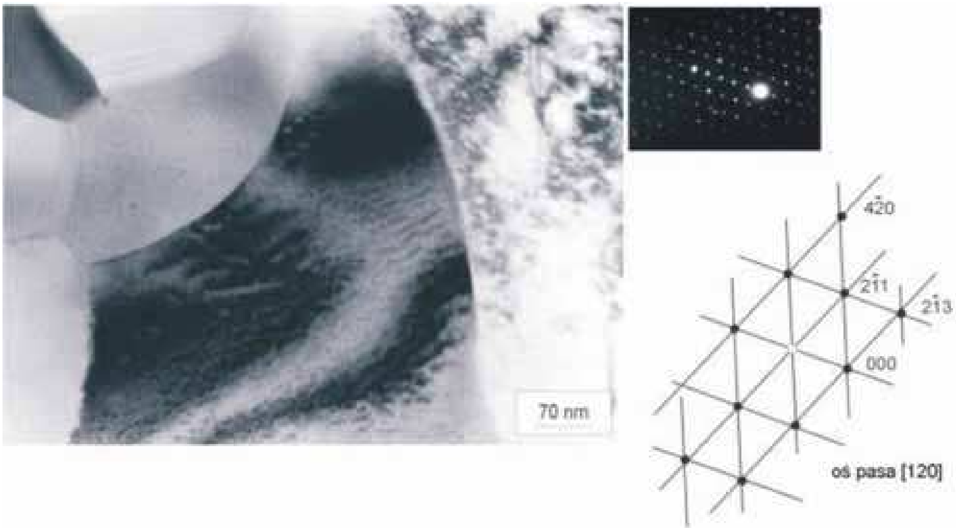

Fig. 8. Microstructure of the AlCu6Ni alloy: particle of α-Al_2CuMg phase

The intermetallic phases S-Al_2CuMg (fig. 7) and α-Al_2CuMg (fig. 8) as well as hardening phase θ'-Al_2Cu (fig. 9-11) were identified in the alloy microstructure by electron diffraction analysis (Pearson, 1967).

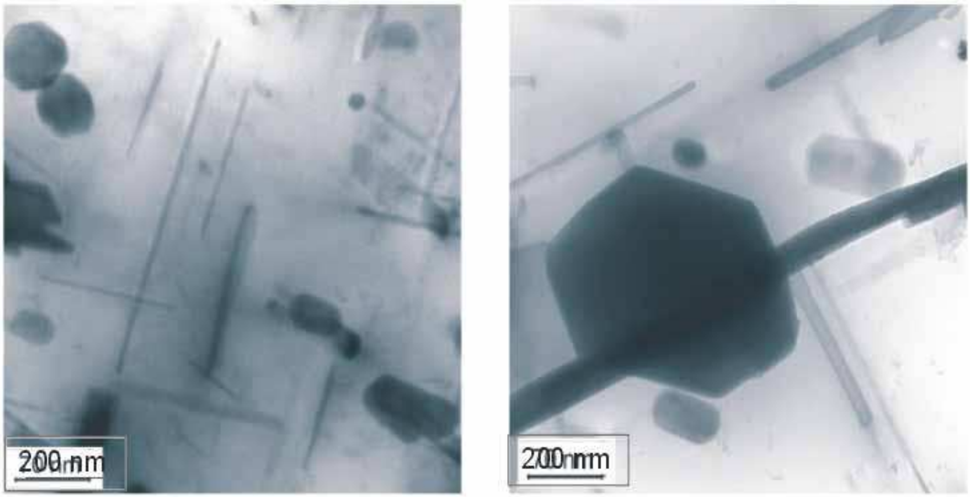

Fig. 9. Microstructure of the AlCu4Ni2Mg alloy in T6 condition (TEM – thin foil). The precipitates of hardening phase θ'-Al_2Cu

Fig. 10. Microstructure of the AlCu6Ni alloy in T6 condition (TEM – thin foil). The precipitates of hardening phase θ'-Al_2Cu

The shape of Al_2Cu particles was diversified from nearly regular polygons – „crystallites" to strongly elongated – "rod-shaped" (fig. 11–12).

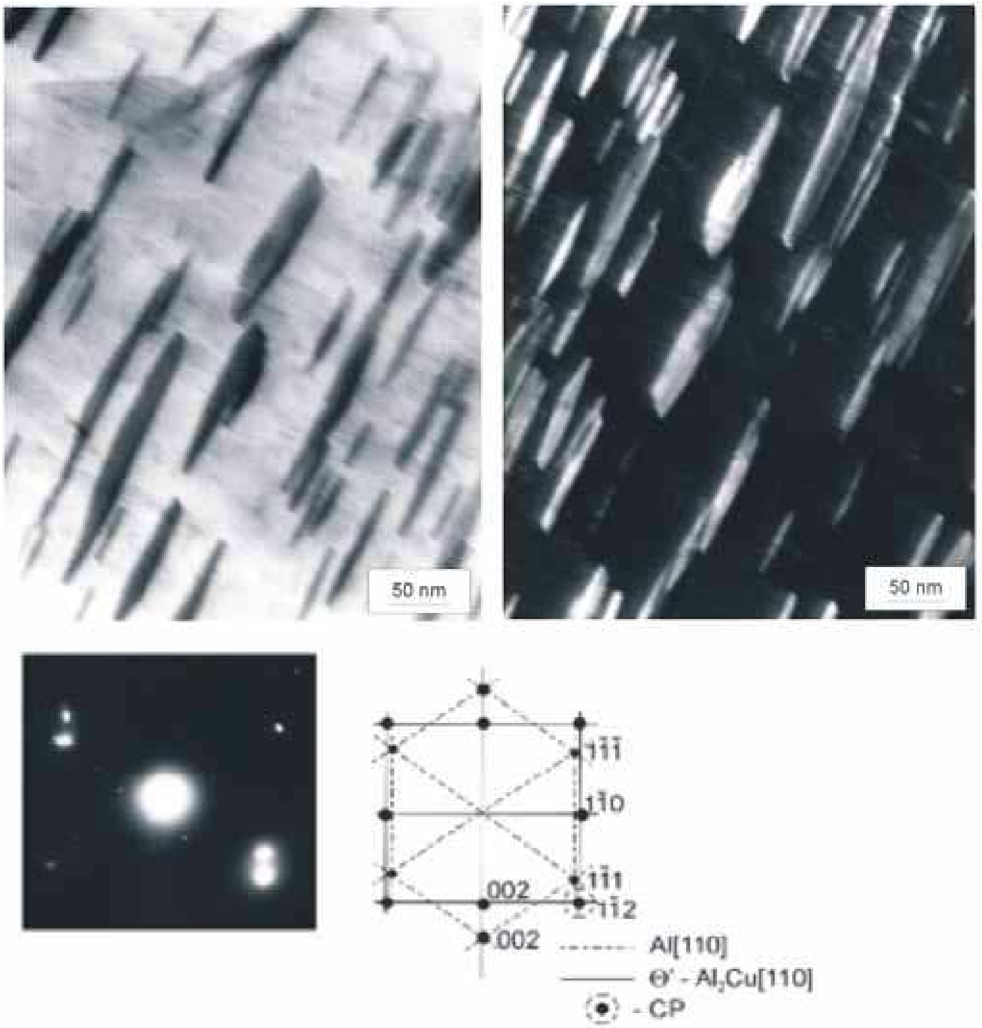

Fig. 11. Microstructure of the AlCu6Ni alloy – precipitates of θ'-Al_2Cu phase in the shape of plates (TEM – thin foil)

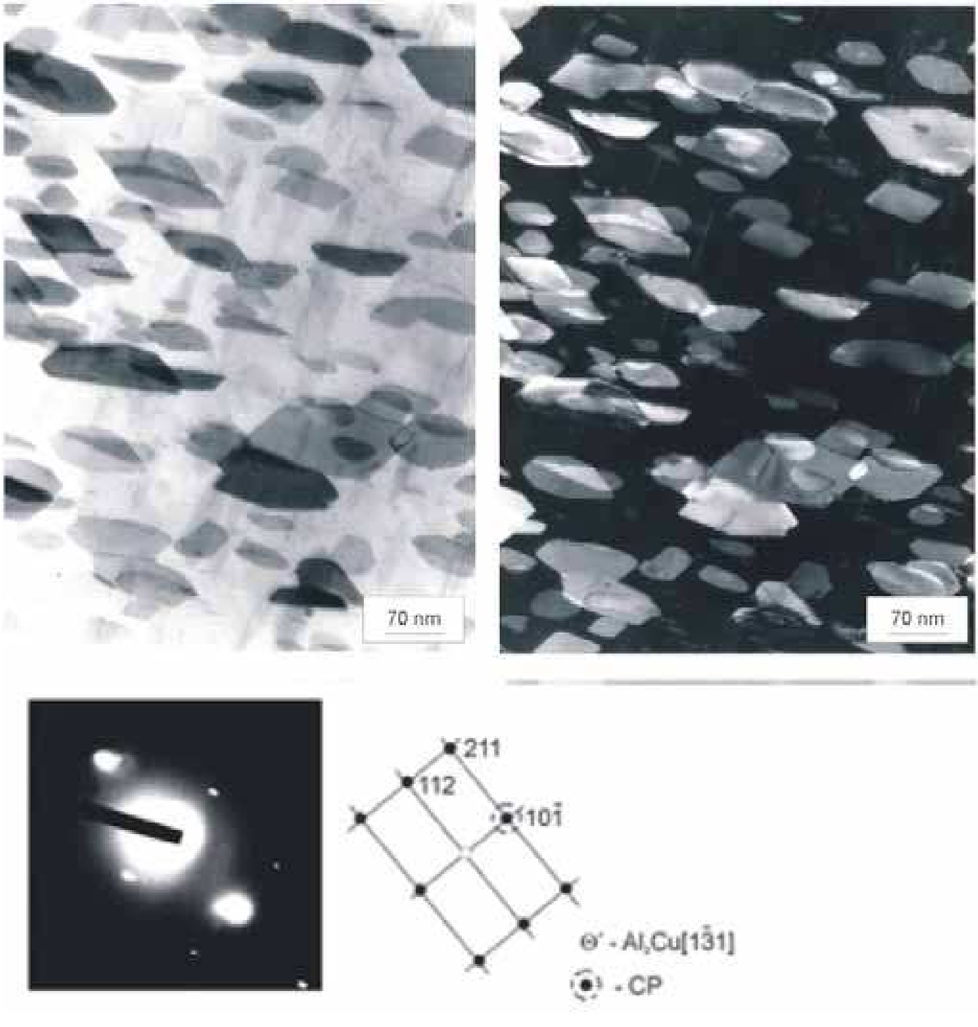

Fig. 12. Microstructure of the AlCu6Ni alloy – precipitates of θ'-Al_2Cu phase in the shape of crystallites (TEM – thin foil)

Examination of the alloys microstructure after prolonged annealing revealed that the precipitates of Al_6Fe and S-Al_2CuMg phases and large precipitates of intermetallic phases at the dendrite boundaries practically did not change (fig. 13–14) even after very long time of annealing (750h). Whereas, significant increase in size of dispersive particles of θ'-Al_2Cu hardening phase was observed (fig. 15-18).

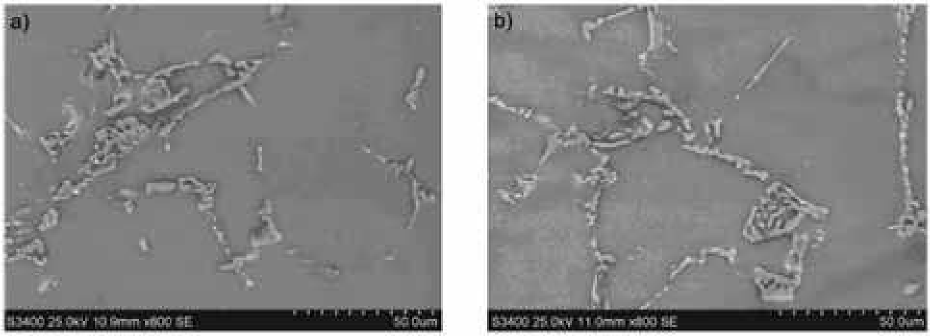

Fig. 13. Microstructure of the AlCu4Ni2Mg alloy after annealing: a) 523K/100h, b) 573K/750h

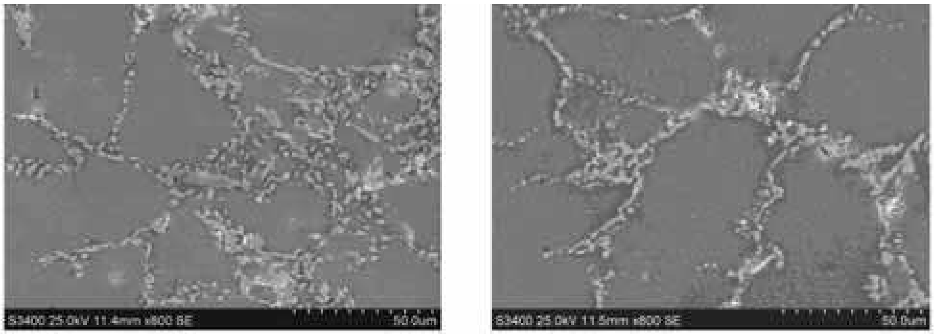

Fig. 14. Microstructure of the AlCu6Ni1 alloy after annealing: a) 523K/100h, b) 573K/750h

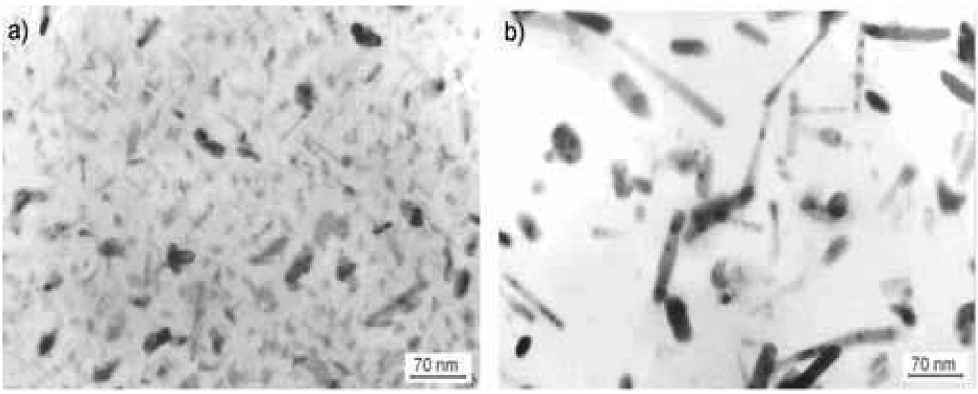

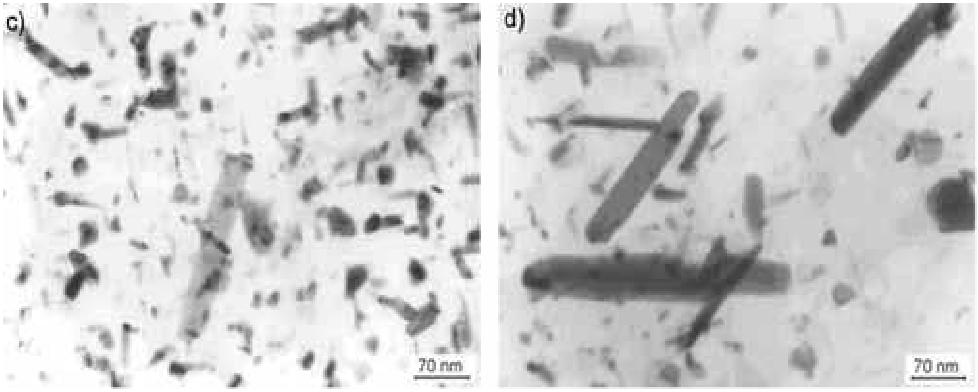

Fig. 15. Microstructure of the AlCu4Ni2Mg alloy – precipitates of the θ′-Al_2Cu phase after annealing at 523 K for: a)100 h, b) 300 h, c) 500 h, d) 750 h

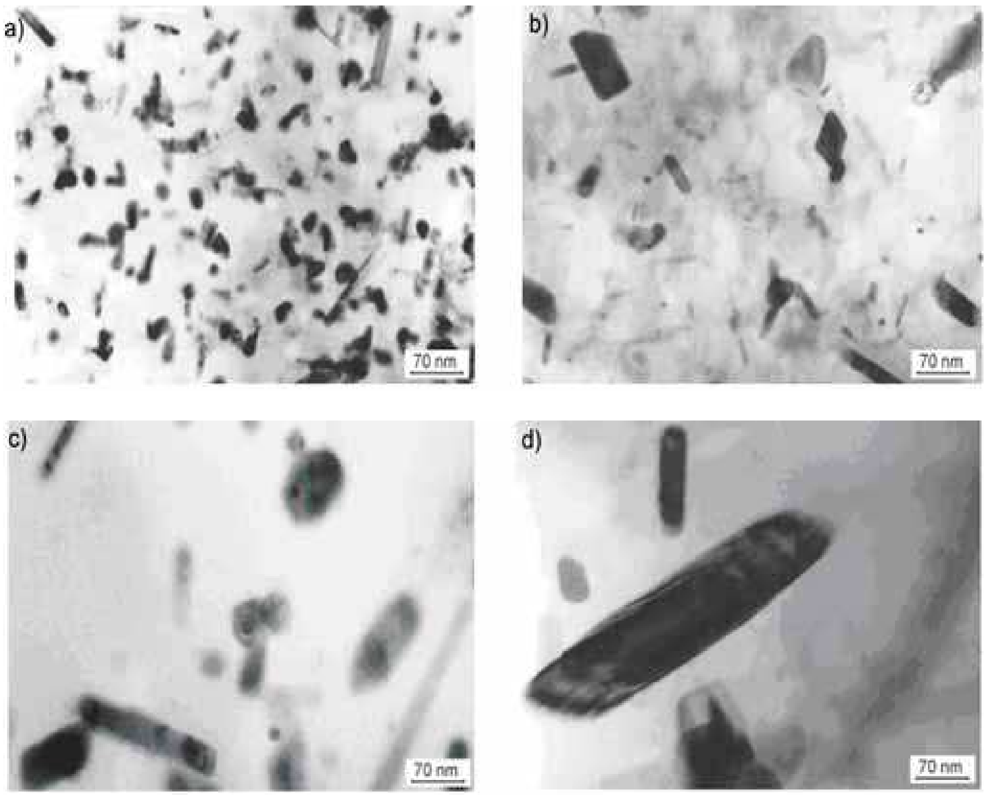

Fig. 16. Microstructure of the AlCu4Ni2Mg alloy – precipitates of the θ′-Al_2Cu phase after annealing at 573K for: a) 100 h, b) 300 h, c) 500 h, d) 750 h

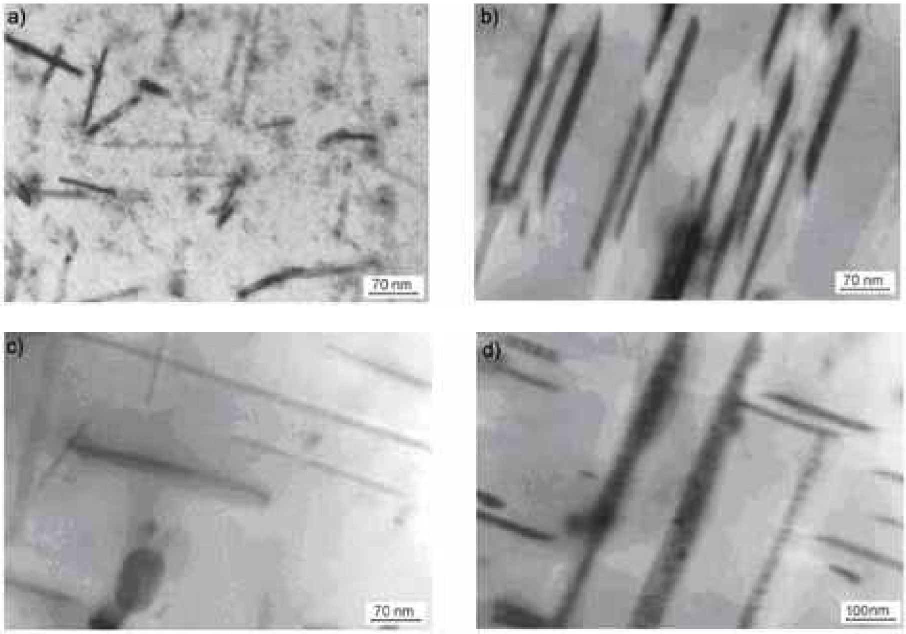

Fig. 17. Microstructure of the AlCu6Ni alloy – precipitates of the θ′-Al_2Cu phase after annealing at 523 K for: a)100 h, b) 300 h, c) 500 h, d) 750 h

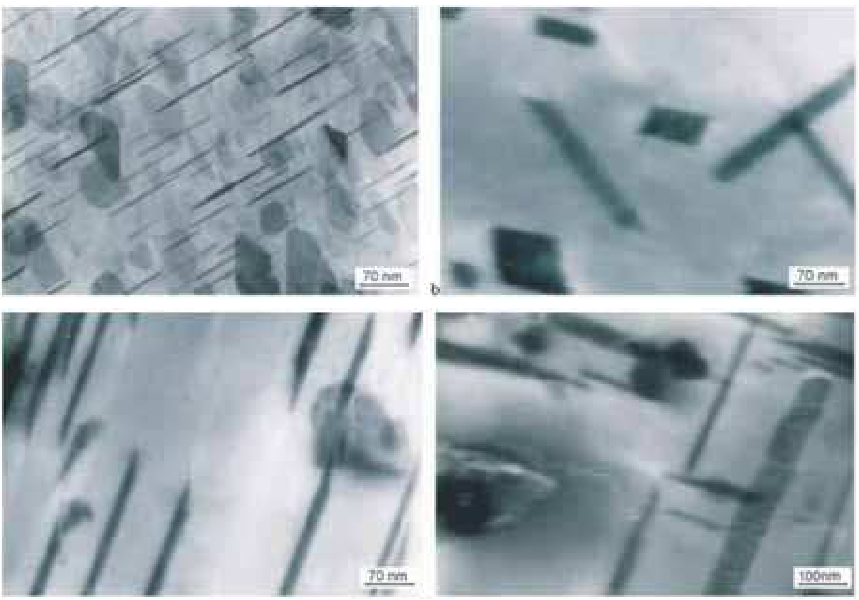

Fig. 18. Microstructure of the AlCu6Ni – precipitates of the θ′-Al_2Cu phase after annealing at 573K for: a) 100 h, b) 300 h, c) 500 h, d) 750 h

Microstructure examination revealed that in both alloys i.e. AlCu4Ni2Mg and AlCu6Ni growth of the hardening phase precipitates occured as a result of long-term thermal loading, which was proportional to the temperature and time of annealing. However higher coarsening propensity was found for Al6CuNi alloy which arose from higher content of the element forming hardening phase (6% Cu). It was confirmed by analysis of the change of shape and size of the θ'-Al_2Cu precipitates in both alloys after annealing at 573K for 150 and 750 h comparing to the standard T6 condition (table 2).

Alloy	Shape parameters of θ′-Al_2Cu precipitates	Heat treatment conditions		
		T6	T6 + annealing at 573 K	
			150 h	750 h
AlCu4Ni2Mg	length, l (nm)	75,12	650,28	887,45
	width, w (nm)	25,20	131,15	158,19
	shape factor l/w	2,98	4,95	5,61
AlCu6Ni	length, l (nm)	55,82	4465,60	6255,05
	width, w (nm)	10,30	115,36	149,11
	shape factor, l/w	5,42	38,71	41,95

Table 2. Evolution of θ′-Al_2Cu precipitates in AlCu4Ni2Mg i AlCu6Ni alloys during annealing at 573K for 150 and 750h

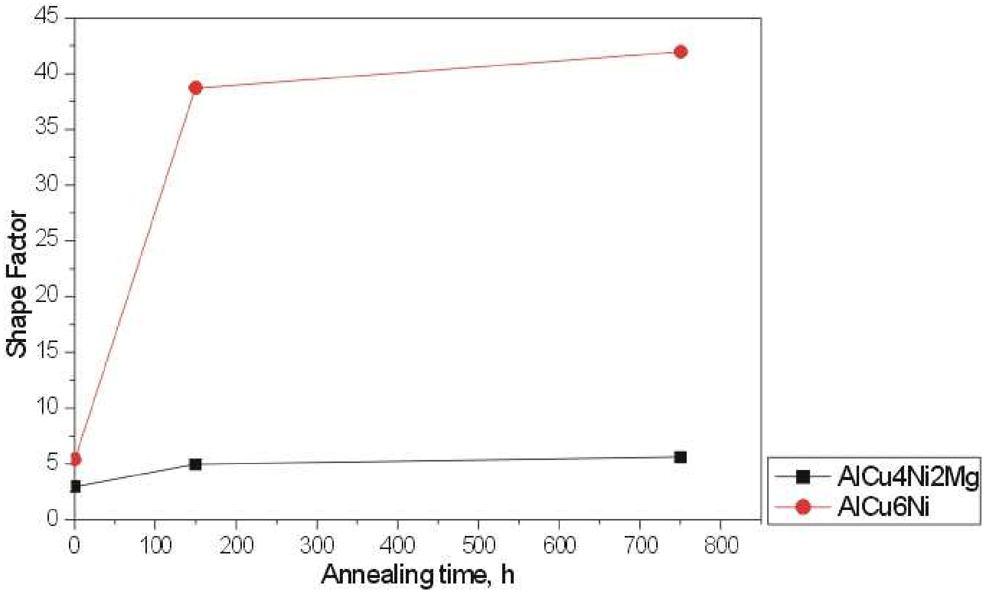

Fig. 19. Change of shape factor of the θ′-Al_2Cu precipitates in AlCu4Ni2Mg and AlCu6Ni as a result of annealing at 573K for 150 and 750h

Results of the measurements showed that annealing of the alloys studied at 573K led to significant growth of hardening θ′-Al_2Cu phase precipitates already after 150h. The biggest change both of size and shape factor of the particles (sevenfold increase) was observed in AlCu6Ni alloy. In the AlCu4Ni2Mg alloy precipitates growth was not so substantial – shape factor was only doubled. Increase in annealing time (750h) resulted in further growth of precipitates. However the process was not so dynamic as in the initial stages of annealing (table 2, fig. 19) – only minor changes of shape factor were observed.
Microstructure examination indicated that growth of the hardening phase precipitates is the main symptom of the microstructure degradation caused by long-term thermal loads. Coarsening and change of the shape of hardening phase particles lead to change of mechanism of their interactions with dislocations and as a consequence of that decrease of strength properties of the alloys (Hirth & Lothe, 1968).
Results of the static tensile test for the alloys studied in T6 condition and after additional annealing at 523 and 573K for 100, 150, 300, 500 and 750h are presented in table 3 and in figures 20 and 21.

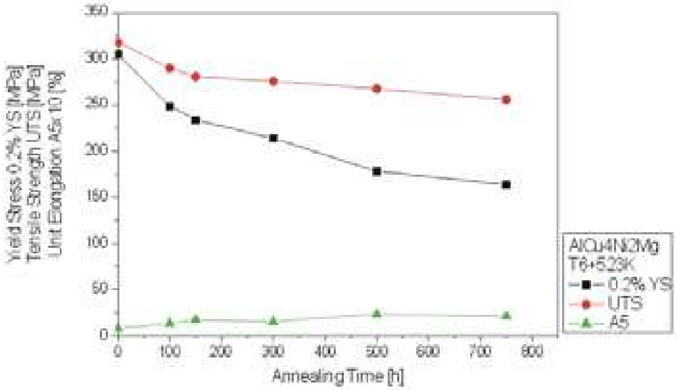

(a)

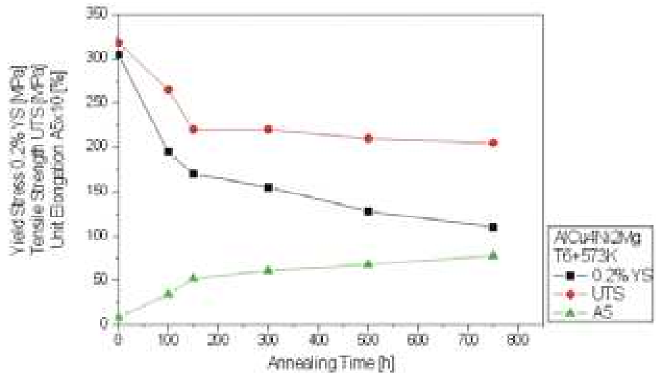

(b)

Fig. 20. Ultimate tensile strength, 0.2% offset yield strength and elongation A_5 for AlCu4Ni2Mg alloy as a function of annealing time at the temperature of a) 523K and b) 573K

Mechanical properties	Heat treatment – temperature and time of annealing										
	T6	T6+523 K					T6+573 K				
		100h	150h	300h	500h	750h	100h	150h	300h	500h	750h
AlCu4Ni2Mg alloy											
0.2%YS, MPa	305	249	234	214	178	164	195	170	155	128	110
UTS, MPa	318	290	281	276	268	256	265	220	220	210	205
A_5, %	0,8	1,3	1,7	1,5	2,3	2,1	3,4	5,2	6,1	6,8	7,8
AlCu6Ni alloy											
0.2%YS, MPa	285	225	215	185	168	142	180	147	140	118	104
UTS, MPa	323	305	290	277	263	243	245	240	216	192	177
A_5, %	0,7	1,3	1,9	2,6	3,1	3,8	2,4	4,2	5,6	6,8	7,0

Table 3. Mechanical properties of the AlCu4Ni2Mg and AlCu6Ni alloys in standard T6 condition and after additional annealing at 523 and 573K

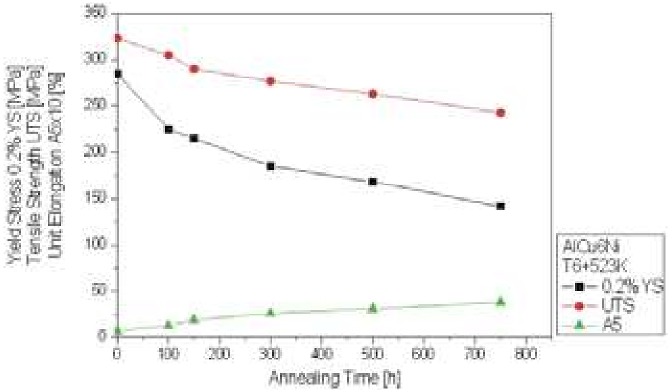

(a)

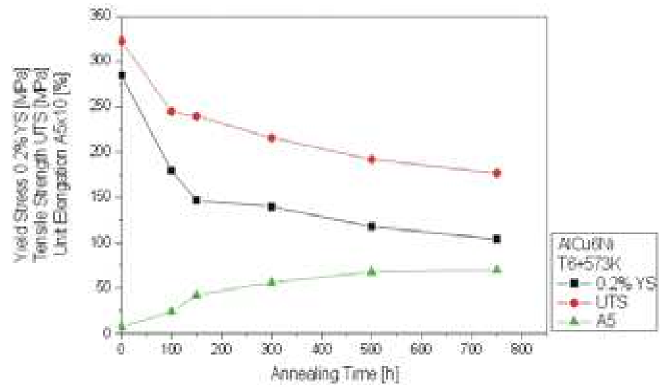

(b)

Fig. 21. Ultimate tensile strength, 0.2% offset yield strength and elongation A_5 for AlCu6Ni alloy as a function of annealing time at the temperature of a) 523K and b) 573 K

Annealing temperature	[(UTS-UTS$_{(T)}$) /UTS] × 100%					[(YS-YS$_{(T)}$) /YS] × 100%				
	100h	150h	300h	500h	750h	100h	150h	300h	500h	750h
	AlCu4Ni2Mg									
523 K	9	12	13	16	19	18	23	30	42	46
573 K	17	31	31	34	35	36	44	49	58	64
	AlCu6Ni									
523 K	5	10	14	19	24	21	25	35	41	50
573 K	24	26	33	40	45	37	48	51	59	64

Table 4. Relative decrease of ultimate tensile strength and 0.2% offset yield strength of the AlCu4Ni2Mg and AlCu6Ni1alloys after annealing at 523 and 573K

It was found that both alloys subjected to long-term annealing exhibit significant reduction of mechanical properties. This tendency was characterized by the coefficient calculated according to the formula $[(R - R_{(T)}) \times R^{-1} \times 100\%]$ where: R – UTS or YS in T6 condition, $R_{(T)}$ – UTS or YS after annealing at 523/573K (table 4). The analysis of the dependence of that

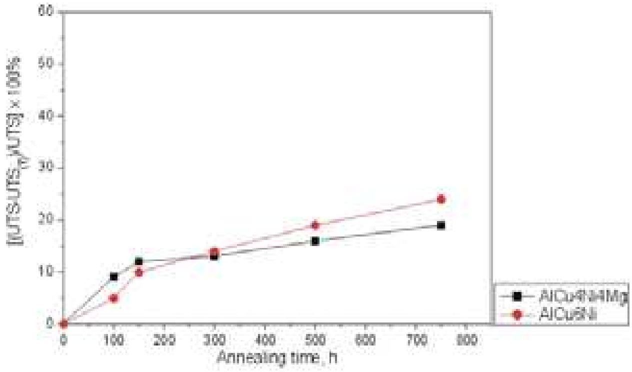

(a)

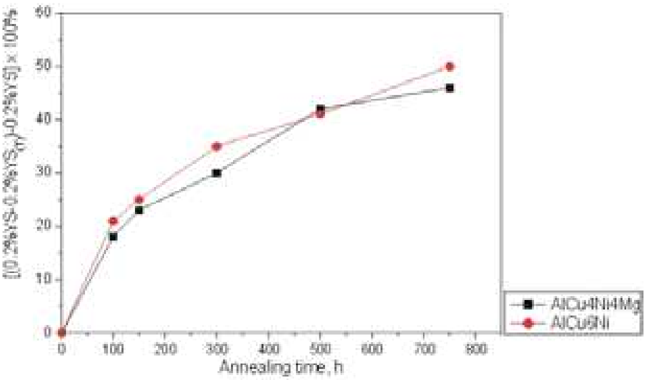

(b)

Fig. 22. Relative change of ultimate tensile strength (a) and 0.2% offset yield strength (b) of the AlCu4Ni2Mg and AlCu6Ni alloys as a function of time of annealing at 523

coefficient value on time of annealing enabled comparison of stability of mechanical properties of the investigated alloys (fig. 22 and 23).

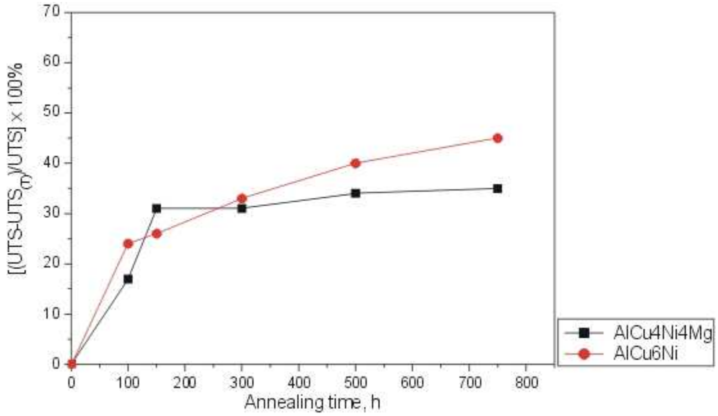

(a)

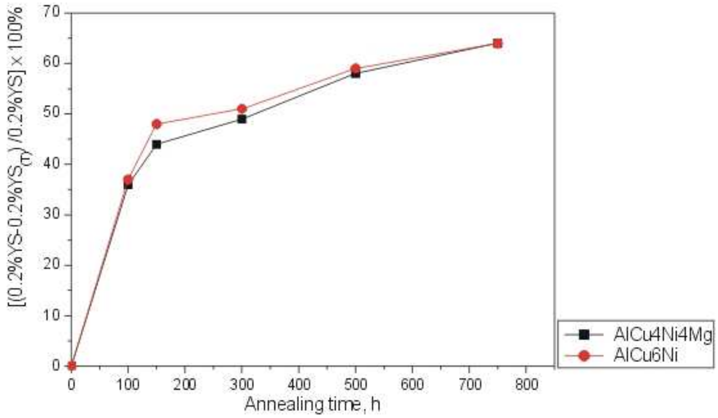

(b)

Fig. 23. Relative change of ultimate tensile strength (a) and 0.2% offset yield strength (b) of the AlCu4Ni2Mg and AlCu6Ni alloys as a function of time of annealing at 573K

Repeatability of the mechanical properties of AlCu4Ni2Mg and AlCu6Ni alloys after long-term annealing was determined on the basis of variation of the static tensile test results (table 5). Five specimens were tested for each temperature and time of annealing. Coefficient of variation was calculated using formula:

$$W_z = \frac{s}{\bar{x}} \times 100 \quad (1)$$

where: s – standard deviation, $\bar{x}$ – average value

Values of the ultimate tensile strength and 0.2% offset yield strength of the alloy subjected to long-term thermal loads (573K/750h) characterize its ability to preserve strength properties in operation condition of the castings (table 5).

Annealing temperature, K	Alloy	0.2% offset yield strength		W_z,%
		$YS_{(max)}$, MPa in T6 condition	$YS_{(min)}$, MPa after annealing for 750h	
523	AlCu4Ni2Mg	305	164	18
	AlCu6Ni	285	142	11
573	AlCu4Ni2Mg	305	110	25
	AlCu6Ni	285	104	18

Table 5. Minimum values of the 0.2% offset yield strength of the AlCu4Ni2Mg and AlCu6Ni alloys after annealing at 523/573K for 750h and maximum values obtained for T6 condition

Both alloys exhibit similar repeatability of tensile test results, however AlCu6Ni alloy shows slightly better stability of strength properties (table 5). However AlCu4Ni2Mg alloy is superior to AlCu6Ni alloy in terms of maximum and minimum yield strength after particular heat treatment. It has also higher ultimate tensile strength.

4. Conclusions

In the AlCu4Ni2Mg and AlCu6Ni alloys degradation of the microstructure takes place as a result of long-term thermal loading. It consists largely in coarsening and the change of the shape of hardening phase particles (θ'-Al_2Cu). The changes are proportional to the annealing time and temperature and lead to significant decrease of the mechanical properties of the alloys. The alloys studied are characterized by different content of Cu – primary element forming hardening phase. Increased Cu content in AlCu6Ni alloy caused only slight improvement of the stability of its strength properties. The AlCu4Ni2Mg alloy containing less Cu but with addition of Mg is characterized by better strength properties than AlCu6Ni alloy in T6 condition and preserves relatively high tensile strength and good ductility after long-term thermal loading. Taking into account criterion of mechanical properties and their stability both alloys studied can be successfully applied for highly stressed elements of aircraft structures operating in the temperature range of 523-573K.

5. References

El-Magd, E. & Dünnwald, J. (1996). Influence of constitution on the high-temperature creep behavior of AlCuMg alloy. *Metallkunde*, Vol.506, pp.411-414

Hirth, J.P. & Lothe, J. (1968). Theory of dislocations. McGraw-Hill, New York-London

Martin, J.W. Preciptation Hardening. (1968). Pergamon Press, Oxford

Mrówka-Nowotnik, G., Wierzbińska, M., & Sieniawski J. Analysis of intermetallic particles in AlSi1MgMn aluminium alloy. (2007). *Journal of Archieves in Materials and Manufacturing Engineering*, Vol.1-2, No.20, pp.155-158

Person, W.B. (1997). A Handbook of Lattice Spacing and Structures of Metals and Alloys, Vol.2, Pergamon Press, Oxford-London-Edinburgh-New York-Toronto-Sydney-Paris-Braunschweig

Wierzbińska, M. & Sieniawski, J. (2010). Microstructural changes to AlCu6Ni1 alliy after prolonged annealing at elevated temperature. *Journal of Microscopy*, Vol.237, No.3, pp.516–520

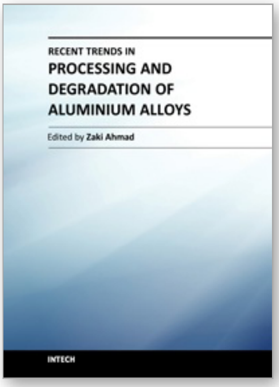

Recent Trends in Processing and Degradation of Aluminium Alloys
Edited by Prof. Zaki Ahmad

ISBN 978-953-307-734-5
Hard cover, 516 pages
Publisher InTech
Published online 21, November, 2011
Published in print edition November, 2011

In the recent decade a quantum leap has been made in production of aluminum alloys and new techniques of casting, forming, welding and surface modification have been evolved to improve the structural integrity of aluminum alloys. This book covers the essential need for the industrial and academic communities for update information. It would also be useful for entrepreneurs technocrats and all those interested in the production and the application of aluminum alloys and strategic structures. It would also help the instructors at senior and graduate level to support their text.